Available online at www.sciencedirect.com

SCIENCE DIRECT®

International Journal of Heat and Mass Transfer 47 (2004) 4415–4425

International Journal of HEAT and MASS TRANSFER

www.elsevier.com/locate/ijhmt

Void fraction predictions in forced convective subcooled boiling of water between 10 and 18 MPa

J.M. Delhaye *, F. Maugin, J.M. Ochterbeck

Department of Mechanical Engineering, Clemson University, Clemson, SC 29634, USA

Received 13 June 2003; received in revised form 25 March 2004

Abstract

Forced convective subcooled boiling is of interest for many industrial applications, especially as a possible heat transfer regime in the core of pressurized water reactors (PWR). Due to practical interest, R12 was used as a testing fluid to simulate water between 10 and 18 MPa. This article presents a study of the forced convective subcooled boiling of R12 based on previous models and new physical considerations. The axial void fraction profile is determined and compared to R12 experimental data obtained on the DEBORA loop at CEA/Grenoble.

The research yielded a void fraction model, shown to be valid for R12 as well as water, and based on a new correlation for the distribution parameter and on a continuous actual quality versus equilibrium quality function extended to the partially developed boiling region. Results showed good agreement with the DEBORA R12 experimental data as well as the experimental data obtained by Bartolomei et al. [Thermal Engng. 29(3) 132] in water at high pressure.

1. Introduction

Forced convective subcooled boiling is of interest for several applications in the power and process industry. In particular, subcooled boiling may be encountered in the core of the pressurized water reactors (PWRs) during startup, nominal or incidental conditions. This boiling flow configuration may lead to a boiling crisis and to burnout of the fuel cladding. Consequently, it is desirable to develop a model able to explain and predict behavior occurring in this type of boiling flow. An experiment performed with steam-water at high pressure to qualify these models would be extremely expensive. As a result, R12 has been used for simulating forced convective subcooled boiling in PWRs. In fact, this fluid can reproduce the same flow characteristics as water in PWR conditions but for a much lower pressure and a much lower heat flux. The following similarity criteria were used (Appendix A):

(a) Identical geometry.
(b) Equivalent vapor/liquid density ratio to determine the corresponding range of pressure:

$$\left(\frac{\rho_g}{\rho_f}\right)_{\text{water}} = \left(\frac{\rho_g}{\rho_f}\right)_{\text{R12}} \tag{1}$$

where ρ_f is the liquid density and ρ_g is the vapor density.
(c) Same Weber number to calculate the corresponding range of mass flux G:

$$We \triangleq \frac{G^2 D}{\sigma \rho_f} \tag{2}$$

where D is the tube diameter and σ is the surface tension.
(d) Same Boiling number to calculate the corresponding range of heat flux Φ:

$$Bo \triangleq \frac{\Phi}{G h_{fg}} \tag{3}$$

where h_{fg} is the latent heat of vaporization.

* Corresponding author. Present address: CEA/Grenoble, DTN/SE2T, 38054 Grenoble Cedex 9, France. Fax: +33-4-38-78-31-96.

E-mail address: jean-marc.delhaye@cea.fr (J.M. Delhaye).

0017-9310/$ - see front matter
doi:10.1016/j.ijheatmasstransfer.2004.05.018

Nomenclature

a	vapor volume at the wall per unit area of the wall
b	expansion ratio (Eq. (18))
Bo	Boiling number (Eq. (3))
C_0	distribution parameter (Eq. (B.3))
C_{01}, C_{02}	Hancox and Nicoll coefficients (Eqs. (24) and (25))
c_p	specific heat
D	tube diameter
Fr	Froude number (Eq. (28))
g	acceleration due to gravity
G	mass flux
h_ℓ	liquid specific enthalpy
h_f	liquid specific enthalpy at saturation
h_{fg}	latent heat of vaporization
j	local volumetric flux of the mixture (Eq. (B.2))
J	mixture volumetric flux
J_g	gas volumetric flux
k	thermal conductivity
L	tube length
L_{cap}	capillary length (Eq. (37))
n	Nabizadeh coefficient (Eq. (27))
P	pressure
Pe	Péclet number (Eq. (14))
Pr_ℓ	liquid Prandtl number (Eq. (9))
q''_{cr}	critical heat flux
Re_ℓ	liquid Reynolds number (Eq. (8))
T	temperature
T_{sat}	saturation temperature
$T_{\ell,in}$	inlet liquid temperature
ΔT_{sat}	wall superheat (Eq. (16))
ΔT_{OSV}	liquid subcooling at the onset of significant void (Eq. (13))
v	velocity
$\widetilde{V}_{gj}$	weighted drift velocity (Eq. (B.4))
We	Weber number (Eq. (2))
x	actual quality
x_{eq}	equilibrium quality
z	coordinate along the channel axis

Greek symbols

α	area void fraction
α_g	local void fraction
β	volumetric quality, cone angle
Φ	heat flux
μ	viscosity
ν	kinematic viscosity
ρ	density
σ	surface tension
ξ	constant in the quality function

Subscripts

c	critical
eq	equilibrium
f	saturated liquid
g	saturated vapor
in	inlet
j	relative to the local volumetric flux of the mixture
ℓ	liquid
$\ell 0$	liquid only
ONB	onset of nucleate boiling
OSV	onset of significant void
sat	saturation
v	vapor
w	wall

(e) Same equilibrium inlet quality to find the corresponding range of inlet temperature:

$$x_{eq,in} \triangleq \frac{h_{\ell,in} - h_f}{h_{fg}} \tag{4}$$

where $h_{\ell,in}$ is the liquid inlet specific enthalpy and h_f is the specific enthalpy of saturated liquid.

An experimental facility named DEBORA was built at CEA/Grenoble [1]. The test section (Fig. 1) is a 3.5 m long heated tube with an inner diameter of 19.2 mm. The control parameters are:

- the exit pressure,
- the mass velocity,
- the heat flux, and
- the inlet equilibrium quality,

which are imposed within the ranges corresponding to the PWR flow characteristics (Table 1). The following local, i.e. pointwise, quantities were measured by a two-sensor optical probe:

- void fraction,
- interfacial area concentration,
- bubble center flux,
- bubble diameter,
- bubble Sauter mean diameter, and
- gas velocity.

The wall temperature was measured by means of four thermocouples placed along the tube external wall.

The vapor generation along a heated tube is represented in Fig. 2, where the most significant boundaries and regions are defined, and the longitudinal profiles of

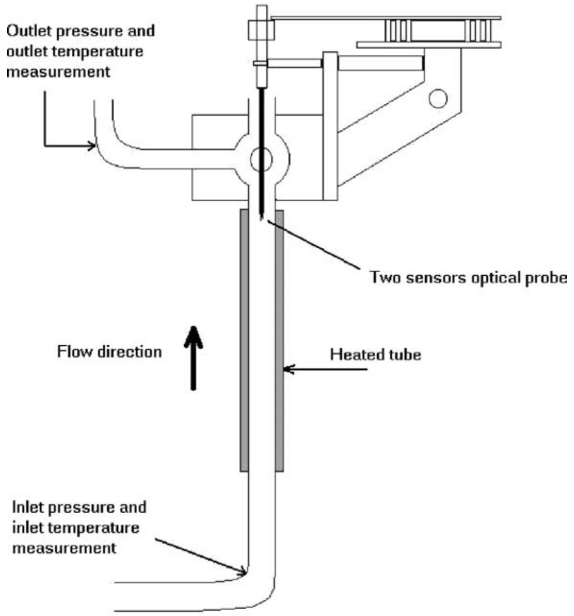

Fig. 1. DEBORA experiment (adapted from [1]).

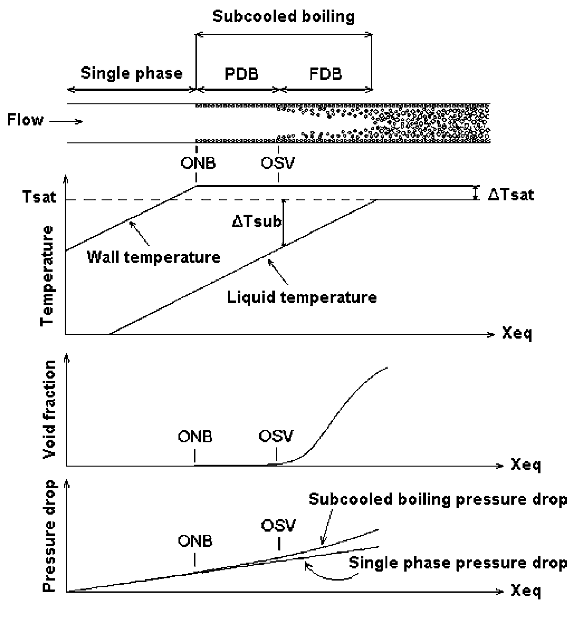

Fig. 2. Forced convective subcooled boiling.

void fraction, pressure drop and wall temperature are schematically represented. The onset of nucleate boiling (ONB) takes place where the first vapor bubbles appear from the nucleation sites. The onset of significant void (OSV) takes place where a significant increase in the void fraction occurs. Finally, forced convective boiling is said to be saturated when the liquid enthalpy reaches the liquid saturation enthalpy. The region between the ONB and the OSV is called the partially developed boiling region (PDB), while the region between the OSV and the saturation state is called the fully developed boiling region (FDB). The void fraction increases slightly from the ONB to the OSV and increases much faster in the FDB region. The pressure drop in this case is higher than the pressure drop in an equivalent single phase flow due to the presence of bubbles. As for the wall temperature, it increases linearly in single phase flow and remains almost constant in the subcooled boiling region.

Table 1
PWR flow characteristics and corresponding R12 flow characteristics of the DEBORA experiment

Parameters	Water	R12
Exit pressure (MPa)	10–18	1.4–3
Mass velocity (kg/m^2 s)	1000–5000	1000–5000
Heat flux (MW/m^2)	0.6–6	0.05–0.65

In the present work, the area void fraction in forced convective subcooled boiling is calculated for imposed values of:

- the mass flux,
- the heat flux,
- the exit pressure, and
- the inlet equilibrium quality.

The void fraction is determined by a model based on the Zuber and Findlay [2] drift flux equation, a new relation between the actual and equilibrium quality and a new correlation for the distribution parameter. The results are then compared to the DEBORA experimental data as well as to the experimental data obtained by Bartolomei et al. [3] in water at high pressure.

2. Significant regime boundaries in subcooled boiling

The onset of nucleate boiling is defined as the point where the first bubbles appear from wall nucleation sites. An energy balance provides its location:

$$z_{\mathrm{ONB}} = \frac{Gc_{p\ell}D}{4}\left[\frac{(T_{\mathrm{sat}} - T_{\ell,\mathrm{in}}) + (\Delta T_{\mathrm{sat}})_{\mathrm{ONB}}}{\Phi} - \frac{1}{h_{\mathrm{fg}}}\right] \tag{5}$$

where

$$\Delta T_{\mathrm{sat}} \triangleq T_{\mathrm{w}} - T_{\mathrm{sat}} \tag{6}$$

The convective heat transfer coefficient, $h_{\ell 0}$, in turbulent liquid flow is given by the Dittus–Boelter correlation:

$$\frac{h_{\ell 0}D}{k_\ell} = 0.023 Re_\ell^{0.8} Pr_\ell^{0.4} \tag{7}$$

where k_ℓ is the liquid conductivity, Re_ℓ and Pr_ℓ are the Reynolds number and the Prandtl number, respectively, and are defined by:

$$Re_\ell \triangleq \frac{GD}{\mu_\ell} \tag{8}$$

$$Pr_\ell \triangleq \frac{\mu_\ell c_{p\ell}}{k_\ell} \tag{9}$$

In Eq. (7) the properties are evaluated at the film temperature $[T_\ell(z_{\mathrm{ONB}}) + T_{\mathrm{w}}(z_{\mathrm{ONB}})]/2$, whereas the liquid specific heat is evaluated at the averaged temperature $[T_\ell(z_{\mathrm{ONB}}) + T_{\ell,\mathrm{in}}]/2$. The wall superheat, $(\Delta T_{\mathrm{sat}})_{\mathrm{ONB}}$, is estimated by the Frost and Dzakowic [4] correlation:

$$(\Delta T_{\mathrm{sat}})_{\mathrm{ONB}} = \left(\frac{8\sigma\Phi T_{\mathrm{sat}}}{k_{\mathrm{f}} h_{\mathrm{fg}} \rho_{\mathrm{v}}}\right)^{0.5} Pr_\ell \tag{10}$$

The properties in Eq. (10) are calculated at the saturation temperature. This correlation, which is known to be reliable for several fluids, is valid for water at pressures from 0.1 to 20 MPa and a heat flux of 0.15 MW/m^2, and for R12 at pressures from 0.1 to 3 MPa and a heat flux of 0.15 MW/m^2. There are no restrictions given about the range of mass flux.

The subcooling, ΔT_{OSV}, at the point where a significant increase in the void fraction appears was determined by Saha and Zuber [5] that has been recognized to be very reliable:

- $Pe < 70000$

$$\Delta T_{\mathrm{OSV}} = 0.0022 \frac{\Phi D}{k_\ell} \tag{11}$$

- $Pe > 70000$

$$\Delta T_{\mathrm{OSV}} = 153.8 \frac{\Phi}{G c_{p\ell}} \tag{12}$$

where

$$\Delta T_{\mathrm{OSV}} \triangleq T_{\mathrm{sat}} - T_\ell(z_{\mathrm{OSV}}) \tag{13}$$

$$Pe \triangleq \frac{GDc_{p\ell}}{k_\ell} \tag{14}$$

A thermal balance then estimates the location of onset of significant void:

$$z_{\mathrm{OSV}} = z_{\mathrm{ONB}} + \{h_\ell[T_\ell(z_{\mathrm{OSV}})] - h_\ell[T_\ell(z_{\mathrm{ONB}})]\} \frac{GD}{4\Phi} \tag{15}$$

3. Void fraction modeling

The void fraction is a parameter of interest because it is required to calculate the pressure drop and because it influences the neutronic response of the reactor core. Levy [6], Kroeger and Zuber [7], Saha and Zuber [5] and Lahey and Moody [8] proposed different methods to calculate the void fraction in subcooled boiling based on the Zuber and Findlay drift flux model (Appendix B). These models differ by the choice of (i) the relation between the actual and equilibrium quality, (ii) the distribution parameter, and (iii) the weighted drift velocity. Also, these models only calculate the void fraction in the fully developed boiling region and assume a zero void fraction in the partially developed boiling region. Levy [6] and Griffith et al. [9] proposed correlations for the void fraction at the OSV, but, to our knowledge, there are no models continuously calculating the void fraction from the ONB to the end of the subcooled boiling region. Manon [10] tested the above quoted models, compared them to the DEBORA experimental data and recommended the use of the Kroeger and Zuber model to calculate the void fraction for forced convective subcooled boiling of R12. However, the results show that this model is actually not very accurate and underestimates the void fraction. In the present work the possibility of improving the Lahey and Moody [8] model was investigated.

3.1. Lahey and Moody model

The objective of the Lahey and Moody [8] model is to estimate the area void fraction in the fully developed boiling region. The calculation is based on the Zuber and Findlay [2] model:

$$\alpha = \frac{x\rho_\ell G}{C_0[x\rho_\ell + (1-x)\rho_{\mathrm{v}}]G + \widetilde{V}_{\mathrm{gj}}\rho_\ell\rho_{\mathrm{v}}} \tag{16}$$

where C_0 is the distribution parameter given by Dix [11]:

$$C_0 = \beta\left[1 + \left(\frac{1}{\beta} - 1\right)^b\right] \tag{17}$$

with

$$b \triangleq \left(\frac{\rho_{\mathrm{v}}}{\rho_\ell}\right)^{0.1} \tag{18}$$

where the volumetric quality, β, is given by:

$$\beta = \frac{x}{x + (1-x)\rho_{\mathrm{v}}/\rho_\ell} \tag{19}$$

The weighted drift velocity, $\widetilde{V}_{\mathrm{gj}}$, is given by:

$$\widetilde{V}_{\mathrm{gj}} = 1.41\left[\frac{\sigma g(\rho_\ell - \rho_{\mathrm{v}})}{\rho_\ell^2}\right]^{1/4} \tag{20}$$

The quality x is calculated as a function of the equilibrium quality x_{eq} according to the Levy [6] suggestion:

$$x(z) = x_{\mathrm{eq}}(z) - x_{\mathrm{eq}}(z_{\mathrm{OSV}}) \exp\left[\frac{x_{\mathrm{eq}}(z)}{x_{\mathrm{eq}}(z_{\mathrm{OSV}})} - 1\right] \tag{21}$$

where z_{OSV} is calculated with the Saha and Zuber model (Eqs. (11)–(15)) and where the equilibrium quality is defined as:

$$x_{eq} \triangleq \frac{h_\ell - h_f}{h_{fg}} \quad (22)$$

As Lahey and Moody did not propose any correlation for the quality in the partially developed boiling (PDB) region between the ONB and the OSV, the void fraction in this region was assumed equal to 0 for all tests. Fig. 3 shows a comparison between the Lahey and Moody model and the DEBORA experimental data for R12. The comparison shows that for R12 the Lahey and Moody model overestimates the value of void fraction in the fully developed boiling region. Consequently, modifications to this model were desired to improve the agreement with the experimental data. Calculations showed that a change in the weighted drift velocity $\widetilde{V}_{gj}$ had very little influence on the calculated void fraction. As a result, modifications were focused on the distribution parameter C_0. In addition, a correlation is proposed for the quality in the PDB region to obtain a non-zero void fraction in this region.

3.2. The distribution parameter C_0

Several models have been developed to estimate the value of the distribution parameter C_0 in subcooled boiling. Some of these models are described below and the values are plotted over the range of parameters corresponding to the DEBORA experiment.

Dix [11] proposed to use Eqs. (17)–(19) for C_0 as a function of quality (Fig. 4). The value of C_0 depends on the pressure only and its variation is small between 1.4 and 2.6 MPa for a given void fraction.

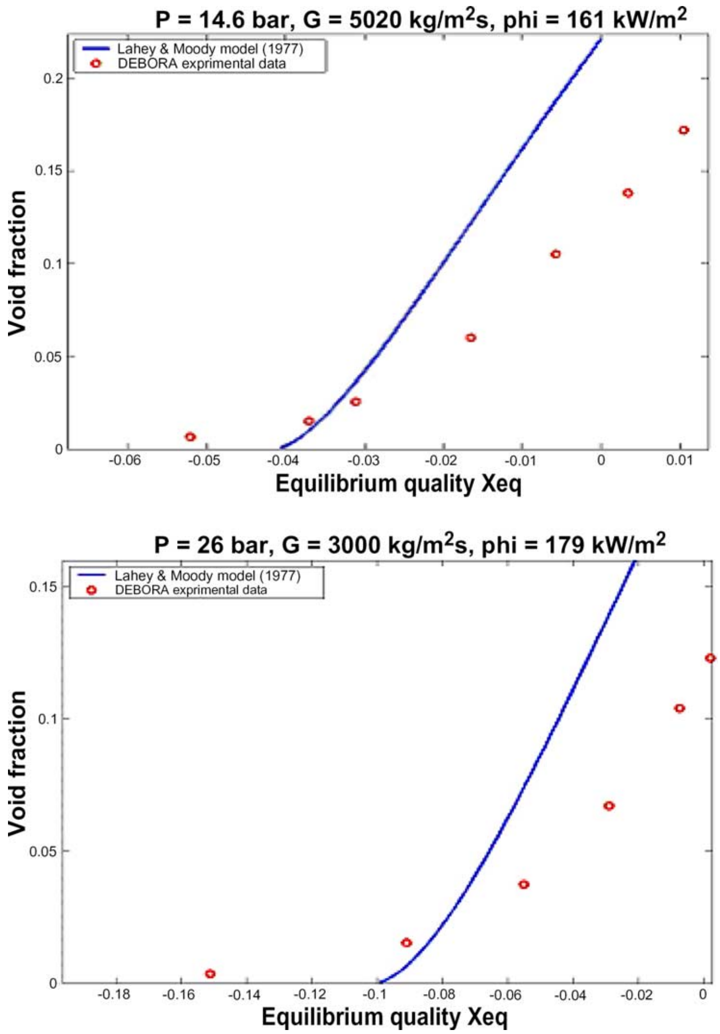

Fig. 3. Comparison between Lahey and Moody model [8] and DEBORA data (R12).

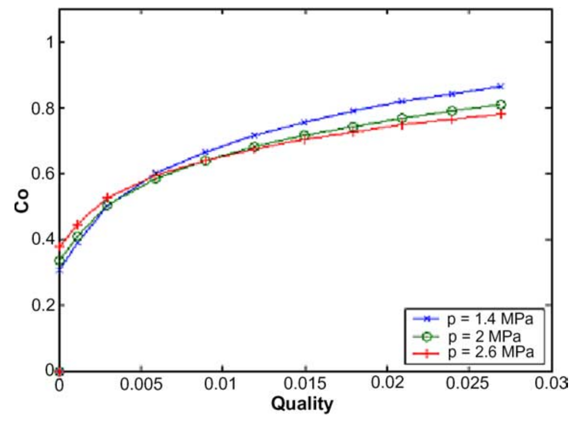

Fig. 4. Distribution parameter in R12 calculated with Dix [11] model.

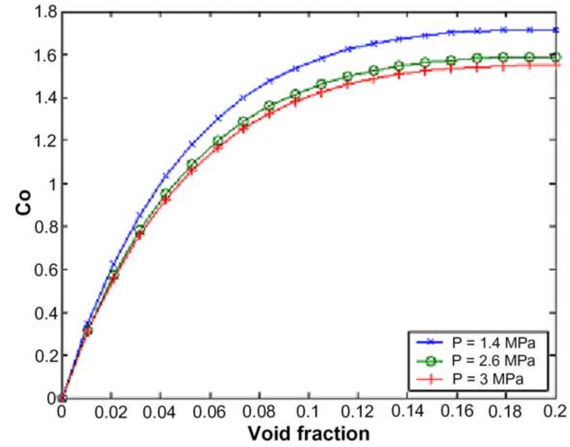

Fig. 5. Distribution parameter in R12 calculated with Hancox and Nicoll [12,13] model.

Hancox and Nicoll [12,13] proposed a value of C_0 depending on the void fraction (Fig. 5):

$$C_0 = \left(\frac{1 - \exp(-C_{01}\alpha)}{1 - \exp(-C_{02})} \right)(1 + C_{02}) - C_{02}\alpha \tag{23}$$

with

$$C_{01} \triangleq 19 \tag{24}$$

$$C_{02} \triangleq 1.164 - 1.6534 \times 10^{-7} P + 7.5086 \times 10^{-15} P^2 \tag{25}$$

where P is in Pa. The C_0 calculated by the Hancox and Nicoll correlation [12,13] depends only on the pressure and the variations are small between 1.4 and 3 MPa. However, the values are too high, as Hoffman and Wong [14] already noticed.

Saha and Zuber [5] assumed that C_0 was a constant equal to 1.13. However, C_0 is not a constant for subcooled boiling since the void fraction and the velocity profiles are not fully developed.

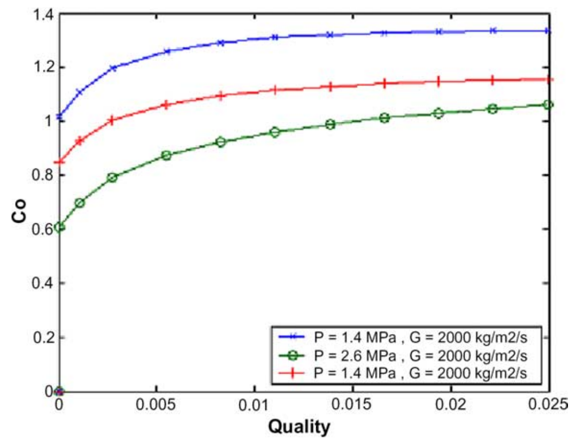

Fig. 6. Distribution parameter in R12 calculated with Nabizadeh [15] model.

Nabizadeh [15] proposed a correlation for C_0 involving the pressure, the mass flux and the quality (Fig. 6):

$$C_0 = \left(1 + \frac{1-x}{x} \frac{\rho_v}{\rho_\ell}\right)^{-1} \left[1 + \frac{1}{n} Fr^{-0.1} \left(\frac{\rho_v}{\rho_\ell}\right)^{n} \left(\frac{1-x}{x}\right)^{11n/9}\right] \tag{26}$$

where

$$n \triangleq \sqrt{0.6 \frac{\rho_\ell - \rho_v}{\rho_\ell}} \tag{27}$$

$$Fr \triangleq \frac{G^2}{gD\rho_\ell^2} \tag{28}$$

The Lahey and Moody [8] model was tested against the DEBORA data with the three distribution parameters models described above. The location of the OSV was calculated with Saha and Zuber model (Eqs. (11)–(15)) and the void fraction at the OSV was assumed equal to 0 for these tests. The results are shown in Fig. 7 along with the DEBORA experimental data. The best results were obtained with Hancox and Nicoll model but a deviation still occurs at 1.46 MPa.

To account for the mass flux and heat flux effects, we assumed that the distribution parameter was a function of the Reynolds number and of the Boiling number. A fit on the DEBORA void fraction data led to the following correlation:

$$C_0 = 0.087 \left(\frac{P}{P_c}\right)^{0.8} \frac{Re_\ell^{0.1}}{Bo^{0.28}} \left[1 - \exp\left(-\frac{\alpha}{0.05}\right)\right] \tag{29}$$

where Bo and Re_ℓ are the Boiling number and the liquid Reynolds number defined by Eqs. (3) and (8), respectively. The variations of the distribution parameter are

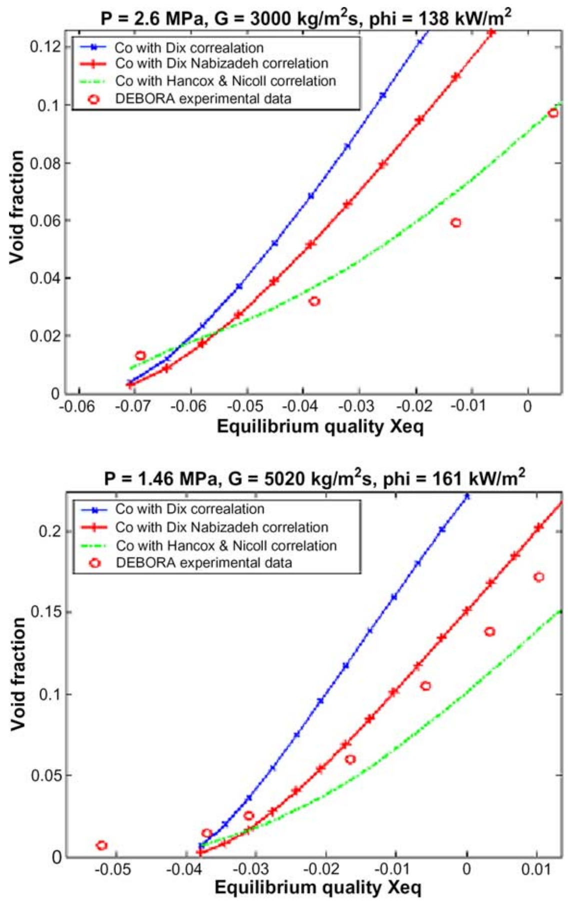

Fig. 7. Comparison between the Lahey and Moody [8] model and the DEBORA data for three different correlations of the distribution parameter.

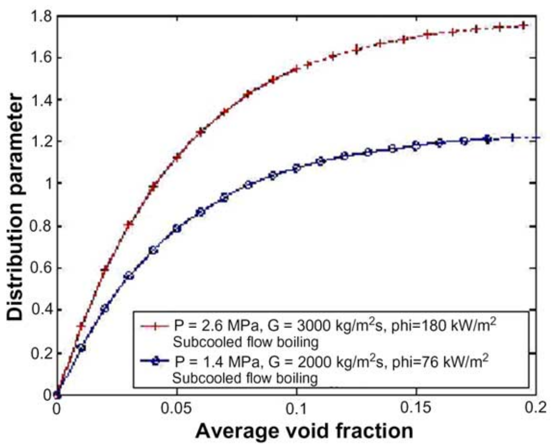

Fig. 8. Distribution parameter calculated with Eq. (29).

represented in Fig. 8. The above C_0 correlation is valid for the following DEBORA parameter ranges:

$$3.4 \times 10^5 < Re_\ell < 8.6 \times 10^5$$

$$2.3 \times 10^{-4} < Bo < 7.2 \times 10^{-4}$$

3.3. Quality in the partial developed boiling region

The Levy model recommended by Lahey and Moody to calculate the quality assumes that the quality is 0 in the PDB region. However, such an assumption is not substantiated by the experimental data.

Facing the inconvenience of the Lahey and Moody model, Manon [10] modified the Levy model to obtain a non-zero value at the OSV:

$$x = x_{eq} + [x_{OSV} - x_{eq}(z_{OSV})] \exp\left[\frac{x_{eq}}{x_{eq}(z_{OSV})} - 1\right] \qquad (30)$$

where x_{OSV} is the quality at the OSV calculated by:

$$x_{OSV} = \frac{1}{2}\frac{\rho_v}{\rho_\ell}\alpha_{OSV} \qquad (31)$$

and α_{OSV} is the void fraction calculated by the Griffith et al. [9] model detailed and modified in Section 3.5. Manon [10] also proposed to use a linear model for the void fraction between the ONB and the OSV.

In order to be more realistic, we propose to represent the quality in the PDB region by a hyperbolic tangent function having a zero derivative at the ONB:

$$x = 0.01\xi\left\{x_{eq} - x_{eq}(z_{ONB})\left\{\tanh\left[\frac{x_{eq}}{x_{eq}(z_{ONB})} - 1\right] + 1\right\}\right\} \qquad (32)$$

where z_{ONB} is the location of the ONB calculated by an energy balance (Eq. (5)) and ξ is a constant to be adjusted in order to allow continuity of the quality between the PDB region and the FDB region. The procedure to adjust ξ is the following:

1. The equilibrium quality for which the derivative of Eqs. (30) and (32) are the same is found by iteration. All tests conducted show that this equilibrium quality is very close to the equilibrium quality at the OSV.

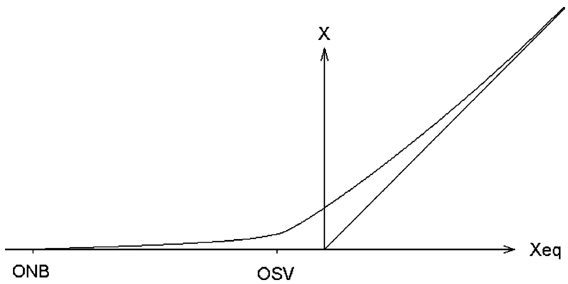

Fig. 9. Quality profile calculated with Eqs. (30) and (32).

2. Then the constant ξ is adjusted so that Eqs. (30) and (32) give the same value of x where their derivatives are equal.

Fig. 9 shows a typical graph of the actual quality, x, versus the equilibrium quality x_{eq}.

3.4. Void fraction at the OSV

To evaluate x_{OSV} it is necessary to determine the void fraction α_{OSV} at the OSV. We suggest to use the Griffith et al. [9] model developed from experimental data obtained for water in the ranges given in Table 2. This model estimates the vapor volume at the wall per unit area of the wall:

$$a = \frac{\Phi k_\ell Pr_\ell}{1.07 h_{\ell 0}^2 [T_{sat} - T_\ell(z_{OSV})]} \quad (33)$$

where the liquid temperature $T_\ell(z_{OSV})$ is estimated by an energy balance between the inlet and z_{OSV}, assuming that the flow is single phase:

$$T_\ell(z) = T_{\ell,in} + \frac{4\Phi z}{G c_{p\ell} D} \quad (34)$$

Table 2
Ranges of experimental data used by Griffith et al. [9]

Parameter	Water	Corresponding ranges in R12
Pressure (MPa)	3.4, 6.9 and 10.3	0.6, 1.2 and 1.8
Mass flux (kg/m^2 s)	80–400	80–400
Heat flux (MW/m^2)	1.6–8.5	0.16–0.93

Table 3
Void fraction at the onset of significant void: comparison between Bartolomei et al. experimental data and Griffith et al. model for void fraction at the OSV

Parameters	Experimental data	Griffith et al. model
$P = 147$ bar $G = 2014$ kg/m^2 s $\Phi = 1720$ kW/m^2	0.02 ± 0.02	0.02
$P = 68.9$ bar $G = 988$ kg/m^2 s $\Phi = 1130$ kW/m^2	0.02 ± 0.02	0.03
$P = 108.1$ bar $G = 966$ kg/m^2 s $\Phi = 1130$ kW/m^2	0.02 ± 0.02	0.03

Table 4
Void fraction at the onset of significant void: comparison between DEBORA experimental data and the modified Griffith et al. model

Parameters	Experimental data	Griffith et al. model	Modified Griffith et al. model
$P = 1.46$ MPa $G = 5020$ kg/m^2 s $\Phi = 135$ kW/m^2	0.01 ± 0.02	0.04	0.01
$P = 1.46$ MPa $G = 5020$ kg/m^2 s $\Phi = 161$ kW/m^2	0.01 ± 0.02	0.04	0.01
$P = 1.45$ MPa $G = 2010$ kg/m^2 s $\Phi = 76.2$ kW/m^2	0.02 ± 0.02	0.06	0.018
$P = 1.46$ MPa $G = 2020$ kg/m^2 s $\Phi = 76.2$ kW/m^2	0.02 ± 0.02	0.06	0.018
$P = 2.62$ MPa $G = 1990$ kg/m^2 s $\Phi = 73.8$ kW/m^2	0.01 ± 0.02	0.05	0.01
$P = 2.6$ MPa $G = 3000$ kg/m^2 s $\Phi = 179$ kW/m^2	0.01 ± 0.02	0.04	0.008
$P = 2.6$ MPa $G = 3000$ kg/m^2 s $\Phi = 138$ kW/m^2	0.01 ± 0.02	0.04	0.008
$P = 2.6$ MPa $G = 3000$ kg/m^2 s $\Phi = 188$ kW/m^2	0.01 ± 0.02	0.04	0.008

where the liquid specific heat, $c_{p\ell}$, is estimated at the temperature $[T_{\ell,\mathrm{in}} + T_\ell(z_{\mathrm{OSV}})]$. The single phase heat transfer coefficient, $h_{\ell 0}$, is determined by the Dittus–Boelter correlation (Eq. (7)). All the liquid properties in Eq. (33) are taken at the OSV temperature. The empirical constant 1.07 was adjusted by the authors on their experimental data. Griffith et al. considered that the partially developed boiling region is governed by the correlation given in Eq. (33) as long as a is lower than 0.1 mm. The void fraction at the OSV, α_{OSV}, is finally given by:

$$\alpha_{\mathrm{OSV}} = \frac{4a}{D} \tag{35}$$

The Griffith et al. model is compared in Table 3 to the experimental data obtained for *water* by Bartolomei et al. [3]. Considering the accuracy of the measurements, the Griffith et al. model gives a good estimate of the void fraction at the OSV. The same model was used with R12 and the results compared to the DEBORA data bank. Table 4 shows that the Griffith et al. model overestimates the value of void fraction at the OSV in R12, which is not surprising since the model was developed for water.

In order to adapt the Griffith et al. model to R12 and to any other fluid, the effect of the surface tension of the fluid was included by introducing the Laplace length in the expression of a:

$$a = 7.5 \frac{\Phi k_\ell Pr_\ell}{h_{\ell 0}^2 (T_{\mathrm{sat}} - T_\ell)} \frac{L_{\mathrm{cap}}}{D} \tag{36}$$

where L_{cap} is the capillary length defined by:

$$L_{\mathrm{cap}} \widehat{=} \sqrt{\frac{\sigma}{g(\rho_\ell - \rho_{\mathrm{v}})}} \tag{37}$$

The modified model gives the same results as the original Griffith et al. model for water and is compared to DEBORA experimental data in Table 4. The comparison shows that the modified Griffith et al. model (Eqs. (35)–(37)) gives a good estimation of α_{OSV}.

3.5. Final model

From the results and discussion above, a new model predicting the evolution of void fraction in subcooled boiling has been developed and is summarized below:

- onset of nucleate boiling (Frost and Dzakowic): Eqs. (5)–(10),
- onset of significant void (Saha and Zuber): Eqs. (11)–(15),
- Zuber and Findlay model: Eq. (16),
- weighted drift velocity: Eq. (20),
- distribution parameter: Eqs. (3), (8) and (29),
- actual quality: Eqs. (30)–(32),
- void fraction at the onset of significant void: Eqs. (34)–(37).

Fig. 10 shows some comparisons between the results obtained with this new model and the DEBORA experimental data. The prediction of the void fraction in the PDB region as well as in the FDB region in forced convective boiling of R12 has been remarkably improved with respect to the Lahey and Moody model (Fig. 3). Most of our results are within the range of accuracy of the DEBORA experiment, which is ±0.02 for the void fraction. In addition, Fig. 11 shows a comparison with Bartolomei et al. [3] experimental data. The model developed also gives a good estimation of the void fraction in forced convective subcooled boiling of water, which further substantiates its physical soundness. Finally, Fig. 12 summarizes all the results obtained for water *and* R12. It shows that the suggested C_0 correlation (29) that was fitted on the DEBORA data can be extended to the Bartolomei et al. data. Consequently,

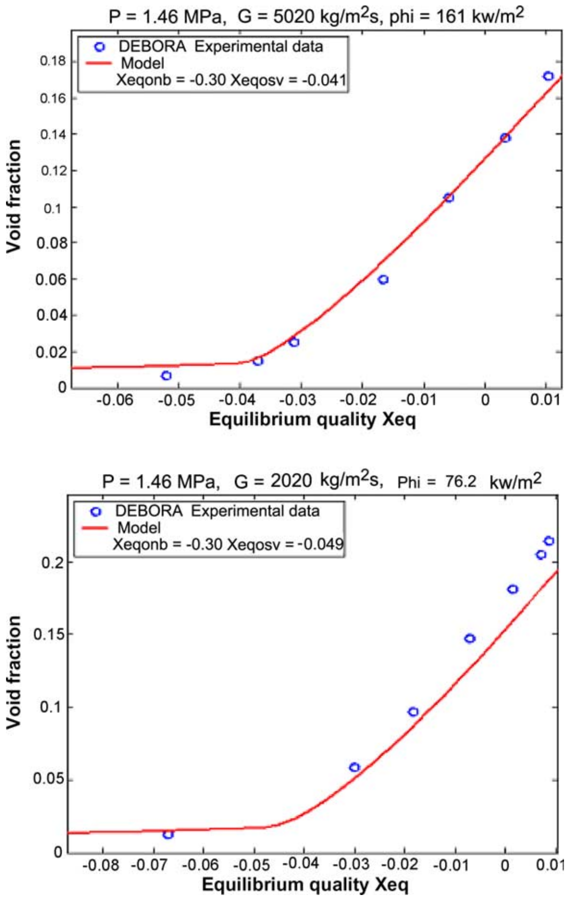

Fig. 10. Comparison between the results of the proposed model and the DEBORA experimental data (R12).

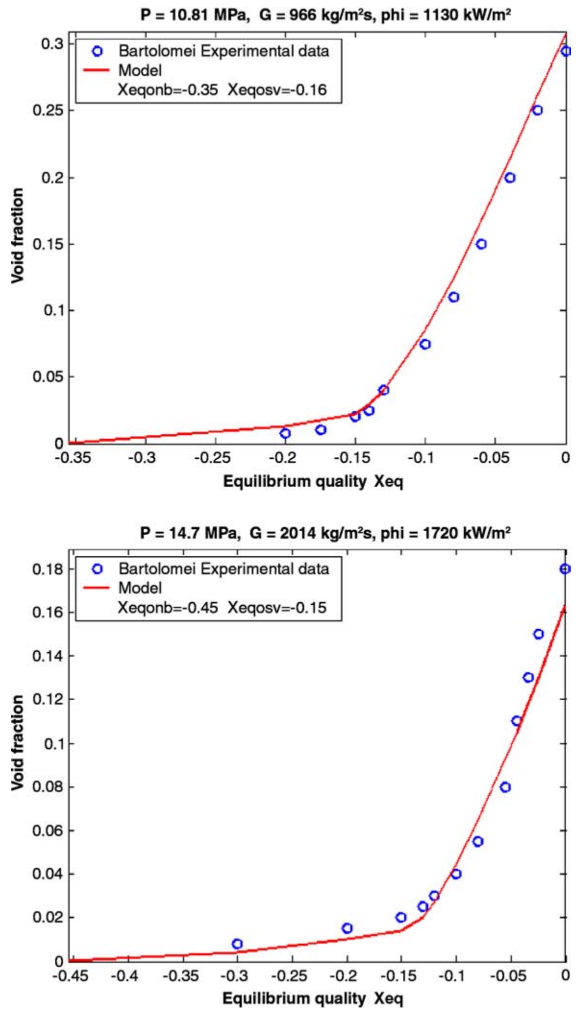

Fig. 11. Comparison between the results of the proposed model and the Bartolomei et al. [3] experimental data (water).

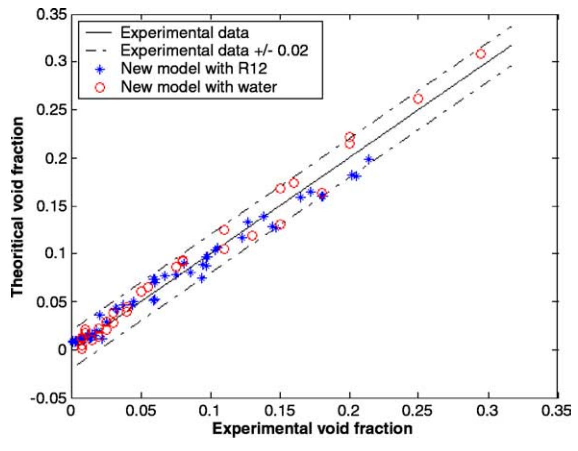

Fig. 12. The proposed model compared to DEBORA (R12) and Bartolomei et al. [3] (water) experimental data.

its validity actually covers the following values of the Reynolds and Boiling numbers:

$$1.4 \times 10^5 < Re_\ell < 8.6 \times 10^5$$

$$2.3 \times 10^{-4} < Bo < 9.4 \times 10^{-4}$$

4. Conclusions

Existing models were adapted and improved in order to calculate the void fraction in forced convective subcooled boiling of R12. A correlation was developed for the distribution parameter used in the Lahey and Moody [8] model. A new equation giving the actual quality versus the equilibrium quality was proposed. The Griffith et al. [9] model giving the void fraction at the onset of significant void was modified and is now valid for water *and* R12. Fig. 12 shows that the proposed void fraction model based on these modified submodels predicts very well the void fraction in subcooled boiling of water *and* R12 within the parameters ranges given in Table 1.

Acknowledgements

This study has been sponsored by EDF (Electricité de France) and CEA (Commissariat à l'Energie Atomique). The authors are fully indebted to Dr. Jacques Garnier, CEA/Grenoble, for his numerous and valuable comments.

Appendix A. Similarity criteria used on Debora

Assume that we have the following functional relationship for the critical heat flux q''_{cr}:

$$q''_{cr} = F(\rho_g, \rho_f, G, D, \sigma, h_{fg}, x_{eq,in}, L)$$

Following Kay and Nedderman [16, pp. 134 et seq.] we can introduce the enthalpy, or thermal energy, as a dimension. A straightforward calculation based on dimensional analysis leads to the five following five dimensionless groups:

- The Boiling number: $Bo \triangleq \frac{\Phi}{Gh_{fg}}$.
- The Weber number: $We \triangleq \frac{G^2 D}{\sigma \rho_f}$.
- The density ratio: ρ_g/ρ_f.
- The aspect ratio: L/D.
- The inlet equilibrium quality: $x_{eq,in}$.

These are the similarity criteria used in Debora.

Appendix B. The Zuber and Findlay model

Zuber and Findlay [17] defined a local drift velocity, v_{gj}, by the following relation:

$$v_{gj} \triangleq v_g - j = (1 - \alpha_g)(v_g - v_f) \tag{B.1}$$

where α_g, v_g and v_f are the local void fraction, the local gas velocity and the local liquid velocity, respectively, and where j is the local volumetric flux of the mixture defined as:

$$j \triangleq \alpha_g v_g + (1 - \alpha_g) v_f \tag{B.2}$$

This relation can also be written as:

$$\alpha_g v_{gj} = \alpha_g v_g - \alpha_g j$$

The Zuber and Findlay equation is obtained by taking the average of the previous relation over the pipe cross section and reads:

$$\alpha = \frac{J_g}{C_0 J + \widetilde{V}_{gj}}$$

It gives the area void fraction, α, as a function of the gas and mixture volumetric fluxes J_g and J if the two following quantities are known:

- The distribution parameter, C_0, defined as:

  $$C_0 \triangleq \frac{\langle \alpha_g j \rangle}{\langle \alpha_g \rangle \langle j \rangle} \tag{B.3}$$

  which depends strongly on the radial profile of the local void fraction, hence its importance in subcooled boiling.
- The weighted drift velocity, $\widetilde{V}_{gj}$,

  $$\widetilde{V}_{gj} = \frac{\langle \alpha_g v_{gj} \rangle}{\langle \alpha_g \rangle} \tag{B.4}$$

  which also depends strongly on the radial profile of the local void fraction.

The distribution parameter and the weighted drift velocity are always determined from experimental database. A direct determination from the definitions would require instrumentation techniques to measure the gas and liquid velocities accurately. Unfortunately these techniques are not yet available.

References

[1] J. Garnier, E. Manon, G. Cubizolles, Local measurements on flow boiling of refrigerant 12 in a vertical tube, Multiphase Sci. Technol. 13 (2001) 1–111.

[2] N. Zuber, J.A. Findlay, Average volumetric concentration in two phase flow systems, J. Heat Transfer 87 (1965) 453–467.

[3] G.G. Bartolomei, V.G. Brantov, Yu.S. Molochnikov, Yu.V. Kharitonov, V.A. Solodkii, G.N. Batashova, V.N. Mikhailov, An experimental investigation of true volumetric vapour content with subcooled boiling in tubes, Thermal Engng. 29 (3) (1982) 132–135.

[4] W. Frost, G.S. Dzakowic, An extension of the method of predictive incipient boiling on commercially finished surfaces, in: ASME-AIChE Heat Transfer Conference, Seattle, 1967.

[5] P. Saha, N. Zuber, Point of net vapor generation and vapor void fraction in subcooled boiling, in: Fifth Int. Heat Transfer Conf., Tokyo, Paper B4.7, 1974.

[6] S. Levy, Forced convection subcooled boiling-prediction of vapor volumetric fraction, Int. J. Heat Mass Transfer 19 (1) (1967) 99–113.

[7] P.G. Kroeger, N. Zuber, An analysis of the effects of various parameters on the average void fractions in subcooled boiling, Int. J. Heat Mass Transfer 11 (1968) 211–233.

[8] R.T. Lahey Jr., F.J. Moody, The Thermal Hydraulics of a Boiling Water Nuclear Reactor, American Nuclear Society, LaGrange Park, IL, 1977.

[9] P. Griffith, J.A. Clark, W.M. Roshenow, Void volumes in subcooled boiling systems, ASME Paper 58-HT-19, ASME, New York, 1958.

[10] E. Manon, Contribution à l'analyse et à la modélisation locale des écoulements bouillants sous-saturés dans les conditions des réacteurs a eau sous pression, Thèse de doctorat, Ecole Centrale de Paris, 2000.

[11] G.E. Dix, Vapor Void Fractions for Forced Convection with Subcooled Boiling at Low Flow Rate, Ph.D. Thesis, University of California, 1971.

[12] W.T. Hancox, W.B. Nicoll, Forced convection boiling; prediction of axial void distributions, Submitted for publication in the Can. J. Chem. Engng., quoted in Hancox and Nicoll [13].

[13] W.T. Hancox, W.B. Nicoll, A general technique for the prediction of void distributions in non-steady two-phase forced convection, Int. J. Heat Mass Transfer 14 (3) (1971) 1377–1394.

[14] M.A. Hoffman, C.F. Wong, Prediction of pressure drops in forced convection subcooled boiling water flows, Int. J. Heat Mass Transfer 35 (12) (1992) 3291–3299.

[15] H. Nabizadeh, Ubertragungsgesetze für den Dampfvolumenanteil zwischen Freon und Wasser, Kolloquium über Aehnlichkeitsgesetze in Zweiphasenströmungen, Institut für Verfahrenstechnik der T.U. Hannover.

[16] J.M. Kay, R.M. Nedderman, An Introduction to Fluid Mechanics and Heat Transfer, third ed., Cambridge University Press, Cambridge, 1974, p. 134 et seq.

[17] N. Zuber, J.A. Findlay, J. Heat Transfer (1965) 453–458.